PROBING THE SHORT-RANGE DYNAMICS IN EXCLUSIVE SCATTERING OFF POLARIZED DEUTERON

MISAK M. SARGSIAN

Department of Physics, Florida International University, Miami, FL 33199

Employing the polarization degrees of freedom in the deuteron allows to isolate smaller than average inter-nucleon distances in the deuteron. As a result one can identify set of high Q^2 reactions off polarized deuteron which are particularly sensitive to the short range dynamics of strong interaction. We concentrate on the studies of several aspects of the short range phenomena. These are the relativistic dynamics of electron–bound-nucleon scattering, color coherence in high Q^2 electro-production as well as the formation of the vector mesons in coherent electro-production from the deuteron. We address also the issue of extraction of polarized deep inelastic structure function of the neutron.

1. Introduction

The deuteron is the simplest nuclear system, which is barley bound with the rms radius of about $4\ fm$. This fact in the momentum space is reflected in the very steep momentum distribution of the unpolarized deuteron wave function with the strength concentrated predominantly at the small internal momenta, Fig.1. However the fact that the deuteron has a D wave which vanishes at small momenta indicates that isolating the D wave in any given nuclear reaction with the deuteron as a target will allow effectively suppress the small-momentum/long-range contributions. This can be seen from the polarized density matrices of the deuteron¹:

$$\rho_{d}^{\vec{a}}(k_{1}, k_{2})) = u(k_{1})u(k_{2}) + \left[1 - \frac{3|k_{2} \cdot a|^{2}}{k_{2}^{2}}\right] \frac{u(k_{1})w(k_{2})}{\sqrt{2}} + \left[1 - \frac{3|k_{1} \cdot a|^{2}}{k_{1}^{2}}\right] \frac{u(k_{2})w(k_{1})}{\sqrt{2}} + \left(\frac{9}{2} \frac{(k_{1} \cdot a)(k_{2} \cdot a)^{*}(k_{1} \cdot k_{2})}{k_{1}^{2}k_{2}^{2}} - \frac{3}{2} \frac{|k_{1} \cdot a|^{2}}{k_{1}^{2}} - \frac{3}{2} \frac{|k_{2} \cdot a|^{2}}{k_{2}^{2}} + \frac{1}{2}\right) w(k_{1})w(k_{2}), \tag{1}$$

where u(k) and w(k) represent the S and D partial waves respectively. The polarization vector \vec{a} is defined through the deuteron spin wave functions:

$$\psi^{10} = i \cdot a_z, \ \psi^{11} = -\frac{i}{\sqrt{2}}(a_x + ia_y), \ \psi^{1-1} = \frac{i}{\sqrt{2}}(a_x - ia_y),$$
 (2)

where $\psi^{1\mu}$ is the projection of the deuteron's spin on the μ direction. The unpolarized density matrix of the deuteron is defined as: $\rho_d^{unp}(k_1, k_2) = \frac{1}{3} \sum_a \rho_d^a(k_1, k_2)$. Since $\lim_{p\to 0} w(p) = 0$, it follows from Eq.(1) that any

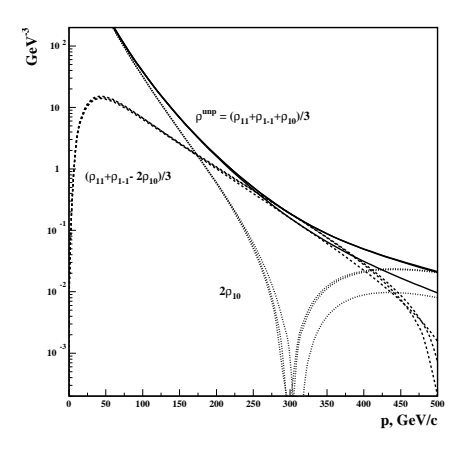


Figure 1. Momentum dependencies of different combination of polarized density matrices. Solid, dashed and doted curves correspond to unpolarized, tensor polarized and transverse polarized distributions respectively.

polarization combination of $\rho_d^{\vec{a}}$, in which u^2 term is canceled has an enhanced sensitivity to the larger internal momenta (smaller distances) of the deuteron as compared to the unpolarized case. As it follows from Eq.(1), the $u(k_1)u(k_2)$ term does not depend on the polarization vector \vec{a} , thus one can cancel this term summing any two components of the density matrix and subtracting the doubled value of the third component.

Fig.1 presents the examples of the density matrices for unpolarized $((\rho_{11} + \rho_{1-1} + \rho_{10})/3$, transverse ρ_{10} and tensor polarized $((\rho_{11} + \rho_{1-1} - 2\rho_{10})/3$ deuteron targets as they enter in the impulse approximation term of the $\vec{d}(e,e'p)n$ cross section (in this case $k_1 = k_2 = p$). As it can be seen from Eq.(1) the tensor polarized density matrix depends only on the terms proportional to u(p)w(p) and $w(p)^2$ which results in a substantial suppression of low-momentum part of the density matrix as compared to the unpolarized one.

We will discuss several studies which utilize this unique feature, that choosing special polarization for the deuteron target enhances the shortrange space-time aspects of the reaction under the consideration.

2. Exclusive $e + \vec{d} \rightarrow e' + p + n$ reaction at $Q^2 \ge 1$ GeV^2 .

The density matrices presented in Fig.1 are probed in the electrodisintegration reaction of the polarized deuteron. There are two aspects in studies of these reactions. One corresponds to the kinematics dominated by impulse approximation (IA) which will provide us with the tool for studies of the deuteron properties at small inter-nucleon distances. Another aspect corresponds to the kinematics dominated by final state interactions (FSI) which is a testing ground for studies of the mechanism of FSI at short distances. In general these two contributions are intertwined together and their separation is an important problem.

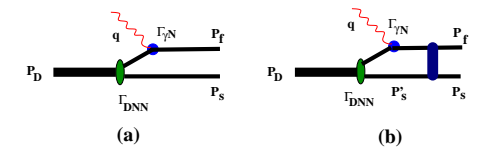


Figure 2. Diagrams for $e + d \rightarrow e' + p + n$ reaction. (a) - IA and (b) FSI contributions.

We discuss d(e, e, p)n reaction in the kinematics in which almost entire momentum of the virtual photon is transferred to the knocked-out nucleon (for certainty we choose it to be a proton) with momentum p_f , while the spectator neutron, with momentum p_s is detected in the momentum range of 0-500 MeV/c. The main kinematic conditions are:

$$Q^2 = \mathbf{q}^2 - q_0^2 > 1 \ GeV^2, \quad \mathbf{p_f} \approx \mathbf{q}, \quad p_f \gg p_m, p_s, \tag{3}$$

where $\mathbf{p_m} = \mathbf{p_f} - \mathbf{q} = -\mathbf{p_s}$ is the missing momentum of the reaction, m is the mass of the nucleon. In the kinematic region of Eq.(3) only the IA (Fig.(2) (a)) and FSI (Fig.(2) (b)) terms will dominate the cross section (see e.g. Ref.^{2,3}). The FSI contribution in $Q^2 \geq 1$ GeV² limit can be calculated within generalized eikonal approximation (GEA)^{1,2,3} which accounts for the finite values of recoil/missing momenta (note that in the Glauber theory the Fermi momenta of interacting nucleons are neglected). With IA and FSI terms included, the differential cross section of $\vec{d}(e,e,p)n$ reaction within distorted wave impulse approximation can be represented as:

$$\frac{d\sigma}{dE_{e'}d\Omega_{e'}d^3p_f} = \sigma_{ep} \cdot S_d^{\vec{s}}(q, p_f, p_s) \cdot \delta(q_o - M_d - E_f - E_s), \tag{4}$$

were σ_{ep} is the cross section of the electron scattering off a bound proton (up to the flux and proton recoil factor) and $S_d^{\vec{s}}(q, p_f, p_s)$ is the distorted spectral function of the deuteron ⁴. Within GEA, for $S_d^{\vec{s}}(q, p_f, p_s)$ one obtains¹

$$S_{d}^{\vec{s}}(q, p_{f}, p_{s}) = \rho_{d}^{\vec{s}}(p_{m}, p_{m}) - \mathcal{R}e \frac{1}{2i} \int \rho_{d1}^{\vec{s}}(p_{m}, p'_{m}) \cdot f^{np}(k_{t}) \cdot \frac{d^{2}k_{t}}{(2\pi)^{2}} + \frac{1}{16} \int \rho_{d2}^{\vec{s}}(p_{m1}, p_{m2}) \cdot f^{np}(k_{t1}) \cdot f^{np*}(k_{t2}) \cdot \frac{d^{2}k_{t1}}{(2\pi)^{2}} \frac{d^{2}k_{t2}}{(2\pi)^{2}} (5)$$

were $\rho_d^{\vec{s}}$ is defined in Eq.(1), whereas $\rho_{d1}^{\vec{s}}$ and $\rho_{d2}^{\vec{s}}$ represent the distorted, due to the re-scattering, density matrices of the deuteron^{1,3}. f^{np} is the amplitude of small angle proton-neutron scattering.

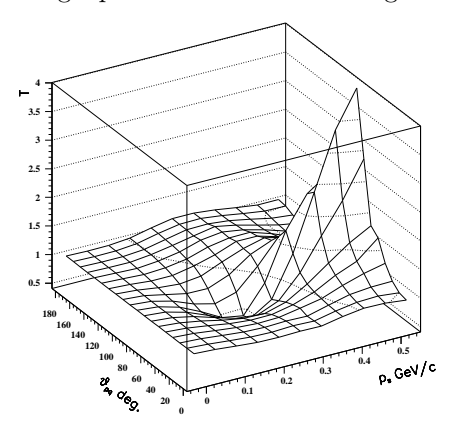


Figure 3. The dependence of the transparency T on the angle - θ_{sq} and the momentum, p_s of the recoil nucleon. The angle is defined with respect to the \mathbf{q} .

To analyze the role of the IA and FSI in the d(e, e'p)n reaction we calculate the ratio of the cross section of Eq.(4) to the cross section calculated within IA only, (Fig.(2(a)):

$$T = \frac{\sigma^{IA+FSI}}{\sigma^{IA}} = \frac{S(p_f, p_s)}{|\psi_D(p_s)|^2}.$$
 (6)

Figure 3 demonstrates the calculation of T as a function of the recoil nucleon angle θ_{sq} with respect to the ${\bf q}$ for the different values of recoil nucleon momentum. It demonstrates the distinctive angular dependence of the ratio T. At recoil nucleon momenta $p_s \leq 300 MeV/c$, T has a minimum and generally T < 1 while at $p_s > 300 MeV/c$, T > 1 and has a distinctive maximum. It can be seen from this picture that the FSI is small at kinematics in which recoil momenta of the reaction is parallel or anti-parallel to ${\bf q}$

(referred to as collinear kinematics). The FSI dominates in the kinematics where $\theta_{pq}\approx 90^0$, more precisely the maximal re-scattering corresponds to the kinematics in which $\alpha\equiv \frac{E_s-p_{sz}}{m}=1$ (referred to as transverse kinematics). The analysis of Fig.3 shows that one indeed can isolate the kinematic domains where IA term is dominant from the domain in which FSI plays a major role. The ability to identify these two kinematics is an important advantage of $e+d\to e'+p+n$ reactions. It allows to concentrate on the different aspects of the dynamics of d(ee'p)n reaction with less background effects. Namely the collinear kinematics are best suited for studies of bound nucleon dynamics while in transverse kinematics one can concentrate on the physics of hadronic re-interaction.

2.0.1. Studies of electro-production from deeply bound nucleons, relativistic effects

The d(e, e'p)n reaction within IA, Fig. 2(a) represents the testing ground for investigation of the electromagnetic structure of bound nucleons. Within IA there is a direct correspondence between the momentum of spectator neutron and the binding energy of the interacting proton $E_b = E_m =$ $m_d - \sqrt{m^2 + p_s^2}$. To achieve such a simplicity in studies of bound nucleon structure, according to the discussions in the previous section, one has to choose collinear kinematics in which FSI is a correction. Additionally, one should restrict the $Q^2 \leq 4 \text{ GeV}^2$ in which case we expect minimal color transparency effects (see next section) and therefore the FSI, being small, are also well under the control. Furthermore, we focus on the parallel kinematics in which the light cone momentum of spectator nucleon, $\alpha \equiv \frac{E_s - p_s^z}{m} > 1$ and $p_{\perp} \approx 0$. The d(e.e'p)n reaction in these kinematics are most sensitive to relativistic effects in the deuteron⁵. The sensitivity to relativistic effects persists also at angles of spectator nucleon momenta close to the collinear kinematics. This sensitivity gradually disappears at $\alpha \to 1$ and $\theta_{sq} \to 90^{\circ}$. There are several techniques for treating the deeply bound nucleons as well as relativistic effects in the deuteron. One group of approaches handles the virtuality of the bound nucleon within a description of the deuteron in the lab. frame (we will call them virtual nucleon (VN) approaches) by taking the residue over the energy of the spectator nucleon. One has to deal with negative energy states which arise for non-zero virtualities (see e.g. Ref.⁶). Due to the binding, the current conservation is not automatic and one has to introduce a prescription to implement electromagnetic gauge invariance (see e.g. Ref.⁷).

Another approach is based on the observation that high energy processes

evolve along the light-cone. Therefore, it is natural to describe the reaction within the light-cone (LC) non-covariant framework 5 . Negative energy states do not enter in this case, though one has to take into account so called instantaneous interactions. For this purpose one employs e.m. gauge invariance to express the "bad" electromagnetic current component (containing instantaneous terms) through the "good" component $J_+^A = -q_+/q_-J_-^A$. In the approximation when non-nucleonic degrees of freedom in the deuteron wave function can be neglected, one can unambiguously relate the light-cone wave functions to those calculated in the Lab frame by introducing the LC pn relative three momentum $k = \sqrt{\frac{m^2 + p_t^2}{\alpha(2-\alpha)} - m^2}$.

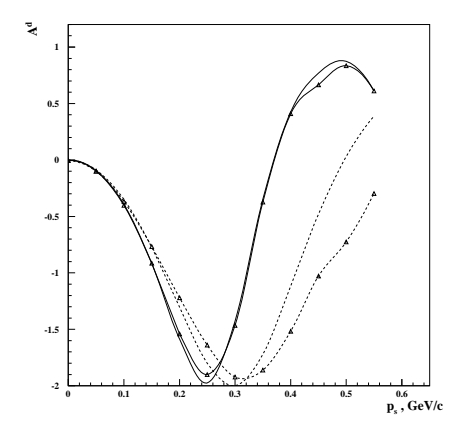


Figure 4. p_s dependence of the d(e, e'p)n tensor polarization asymmetry at $\theta_{sq} = 180^{\circ}$. Solid and dashed lines are IA predictions of the LC and VN methods, respective marked curves include FSI.

Naturally, VN and LC approaches coincide in the limit of small missing momenta. Their predictions within IA considerably diverge at larger values of spectator momenta ($\geq 300 MeV/c$)⁵. According to the discussion in Sec.1 the d(e,e'p)n reactions with a tensor polarized deuteron is best suited for discrimination between VN and LC prescriptions. This was previously demonstrated within IA in Ref.⁵. Using the recent advances in the calculation of FSI, one can perform a similar comparison for asymmetry:

$$A^{d} = \frac{\sigma^{1,1} + \sigma^{1,-1} - 2\sigma^{1,0}}{\sigma^{1,1} + \sigma^{1,-1} + \sigma^{1,0}},\tag{7}$$

accounting also for FSI contribution of Fig.2(b). In Eq.(7) $\sigma^{1,s_z} \equiv \frac{d\sigma^{\vec{s},s_z}}{dE_{e'}d\Omega_{e'}d^3p_s}$ represents the differential cross section of d(e,e'p)n reaction with the deuteron helicity, s_z .

The results of VN and LC comparison which includes both IA and FSI contributions are presented in Fig.4 for collinear kinematics with $\theta_{sq}=180^o$. One can see that account of the FSI further increases the difference between VN and LC predictions, thus making their experimental investigation more feasible.

2.0.2. Color Transparency studies at intermediate Q^2

In QCD, the absorption of a high Q^2 photon by a nucleon produces a point like configuration (PLC), which, at asymptotically high energies, would not interact with the nucleons, thus eliminating FSI. This effect generally is referred as a color transparency (CT). Recently, CT was experimentally observed⁸ in the high energy $\pi + A \rightarrow 2jets + A'$ reactions which confirmed the early prediction based on perturbative QCD (pQCD) calculations⁹.

At high but finite energies (pre pQCD domain), a PLC is actually produced, but it expands as it propagates through the nucleus 10 . To suppress the expansion effects, it is necessary to ensure that the expansion length, $l_h \sim 0.4 (p/\text{GeV})$, is greater than the characteristic longitudinal distance in the reaction. In the considered d(e,e'p)n reaction, where one nucleon carries almost all the momentum of the photon while the second nucleon (or its resonance) is a spectator, the actual expansion distances are the distances between the nucleons in the deuteron 1 . Thus, suppressing large distance effects through the deuteron's polarization, one effectively will diminish the PLC's expansion, leading to an earlier onset of CT.

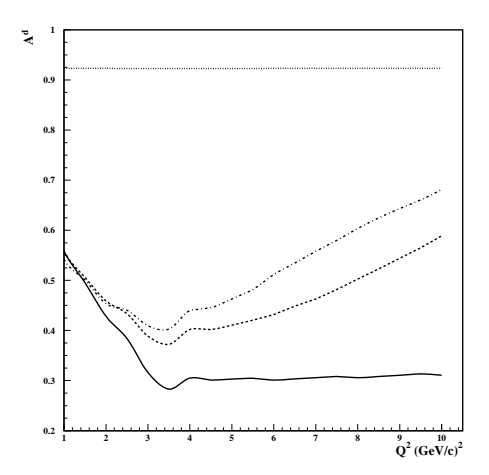


Figure 5. Q^2 dependence of A_d for $\alpha=1.$ Solid line - GEA, dashed - QDM, dashed-dotted - three state model, dotted -PWIA.

The reduced interaction between the PLC and the spectator nucleon can be described in terms of its transverse size and the distance z from the photon absorption point in d(e, e'p)n reaction. As a result the pn rescattering amplitude, f^{pn} , in Eq.(5) is replaced by $f^{PLC,N}(z, k_t, Q^2)$. For numerical estimates of the $f^{PLC,N}(z, k_t, Q^2)$, we use the quantum diffusion model (QDM) ¹¹ as well as the three state model ¹². Latter is based on the assumption that the hard scattering operator acts on a nucleon and produces a PLC, which is represented as a superposition of three baryonic states, $|PLC\rangle = \sum_{m=N,N^*,N^{**}} F_{m,N}(Q^2)|m\rangle$.

To study the expected effect of CT we choose now a transverse kinematics, in which FSI is dominant (see Fig.3 . Furthermore we choose the tensor polarization of the deuteron target which is sensitive to the D wave and therefore FSI will be dominated at smaller inter-nucleon distances. As a result one will probe the evolution of PLC at smaller space-time intervals.

For numerical estimates, we consider the Q^2 dependence of the asymmetry A_d from Eq(7) for fixed and transverse momenta of the spectator neutron. This dependence for $p_t = 300 \text{ MeV/c}$, is presented in Fig.5 One can see from this figure that CT effects can change A_d by as much as factor of two for $Q^2 \sim 10 \text{ GeV}^2$. It is worth noting that the same models predict 15-20% effect for (e, e'p) reactions on unpolarized nuclear targets.

3. Coherent production of vector mesons from polarized deuterons at high Q^2

The ability to select smaller than average inter-nucleon distances in the reactions involving polarized deuteron target is explored further in the reactions of coherent electro-production of vector mesons, i.e. $e+\vec{d} \rightarrow e'+d'+V$, in which V represents a neutral mesons i.e. ρ , ω , ϕ etc.

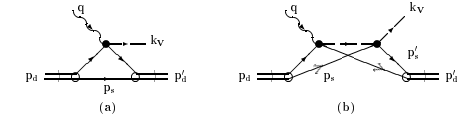


Figure 6. IA (a) and FSI (b) contributions to d(e, e'V)d' reaction.

In this case two, impulse approximation (IA) and single re-scattering diagrams define the overall cross section (see Fig.6). At high Q^2 one may expect that the intermediate state produced by the virtual photon in the FSI amplitude (Fig.6(b)) will be dominated by PLCs. As a result one may observe a diminished re-interaction with the spectator nucleon. The philosophy here is similar to that of deuteron electro-disintegration reaction,

which is too look for specific polarization of target deuteron in order to achieve the highest possible sensitivity to the FSI term contributing to the cross section of the reaction.

To see the role of the deuteron polarization we analyze the production amplitude of $\gamma^* + d \rightarrow d' + V$ reaction, which be written as follows¹³

$$F_{df}^{jj'} = F^{(a)} + F^{(b)} = f^{\gamma^* N \to VN}(\mathbf{l}) \left[S_{df}^{jj'} \left(-\frac{\mathbf{l}_{\perp}}{2}, \frac{l_{\perp}}{2} \right) + S_{df}^{jj'} \left(\frac{\mathbf{l}_{\perp}}{2}, -\frac{l_{\perp}}{2} \right) \right]$$

$$+ \frac{i}{2} \sum_{h} \int \frac{d^2 k_{\perp}}{(2\pi)^2} f^{\gamma^* N \to hN} \left(\frac{\mathbf{l}_{\perp}}{2} - \mathbf{k}_{\perp} \right) f^{hN \to VN} \left(\frac{\mathbf{l}_{\perp}}{2} + \mathbf{k}_{\perp} \right)$$

$$\times \left[S_{df}^{jj'}(\mathbf{k}_{\perp}, -\Delta_h) + \frac{2i}{\sqrt{2\pi}} \Delta S_{df}^{jj'}(\mathbf{k}_{\perp}, -\Delta_h) \right]. \tag{8}$$

where $S_{df}^{jj'}$ is the transition form-factor of the deuteron, $f^{\gamma^*N\to VN}$ and $f^{hN\to VN}$ corresponds to the amplitudes of $\gamma^*+N\to N+h$ and $h+N\to N+V$ reactions respectively. $l_-=l_0-l_z$, where l_0 and $\mathbf l$ are the transferred energy and momentum to the final deuteron. The transition form-factor of the deuteron, S forms the density matrix that enters in the differential cross section of the reaction. In the general form this density matrix can be represented as follows:

$$\begin{split} \rho^{1,m}(\mathbf{l_{1}},\mathbf{l_{2}}) &= \sum_{m'} S_{d}^{s,mm'}(\mathbf{l_{1}}) S_{d}^{1,mm'}(\mathbf{l_{2}})^{\dagger} = F_{C}(l_{1}) F_{C}(l_{2}) \\ &+ \frac{1}{\sqrt{2}} \left\{ \left[\frac{3 |\mathbf{l_{2}} \cdot \epsilon_{\mathbf{1}}^{\mathbf{m}}|^{2}}{l_{2}^{2}} - 1 \right] F_{C}(l_{1}) F_{Q}(l_{2}) + \left[\frac{3 |\mathbf{l_{1}} \cdot \epsilon_{\mathbf{1}}^{\mathbf{m}}|^{2}}{l_{1}^{2}} - 1 \right] F_{C}(l_{2}) F_{Q}(l_{1}) \\ &+ \left[9 \frac{(\mathbf{l_{1}} \cdot \epsilon_{\mathbf{1}}^{\mathbf{m}})(\mathbf{l_{1}} \cdot \epsilon_{\mathbf{1}}^{\mathbf{m}})^{*} \mathbf{l_{1}} \cdot \mathbf{l_{2}}}{l_{1}^{2} l_{2}^{2}} - \frac{3 |\mathbf{l_{1}} \cdot \epsilon_{\mathbf{1}}^{\mathbf{m}}|^{2}}{l_{1}^{2}} - \frac{3 |\mathbf{l_{2}} \cdot \epsilon_{\mathbf{1}}^{\mathbf{m}}|^{2}}{l_{2}^{2}} + 1 \right] \\ &\times \frac{F_{Q}(l_{1}) F_{Q}(l_{2})}{2} \right\}, (9) \end{split}$$

where F_C and F_Q are the charge and quadrupole form-factors of the deuteron and $\epsilon_1^{\mathbf{m}}$ is the polarization vector of the target deuteron with m being the deuteron spin projection on the given quantization axis.

In the IA term the ρ function enters with the argument $\mathbf{l_1} = \mathbf{l_2} = \mathbf{l/2}$. Since our aim is to identify the kinematic regions in which the IA term vanishes and FSI is dominant, we search for those polarizations of the deuteron for which the $\rho^{1,m}(\frac{1}{2})$ has a vanishing values for accessible range of 1. The analysis of the density matrix as it enters in the IA term of the cross section is presented in Fig.7. The figure demonstrates that for transversely polarized deuterons the $\rho^{1,0}(\frac{1}{2})$ vanishes at $l \approx 0.7 \text{ GeV/c}$ which corresponds to $-t \approx 0.5 \text{ GeV}^2$. The existence of the zero in $\rho^{1,m}(\frac{1}{2})$ can be understood in the limit of vanishing l_- , in which case

 $\rho^{s,1}(\frac{\mathbf{l}_{\perp}}{2})=(F_C(l_{\perp}/2)-\frac{1}{\sqrt{2}}F_Q(l_{\perp}/2))^2.$ Since F_c monotonically decreases while F_Q increases from the zero value at $l_{\perp}=0,$ the following equation has a solution $F_C(l_{\perp}/2)=\frac{1}{\sqrt{2}}F_Q(l_{\perp}/2))$ which is found to be at $l_{\perp}\approx 0.7~\mathrm{GeV/c}$. Thus our observation is that one has vanishing IA con-

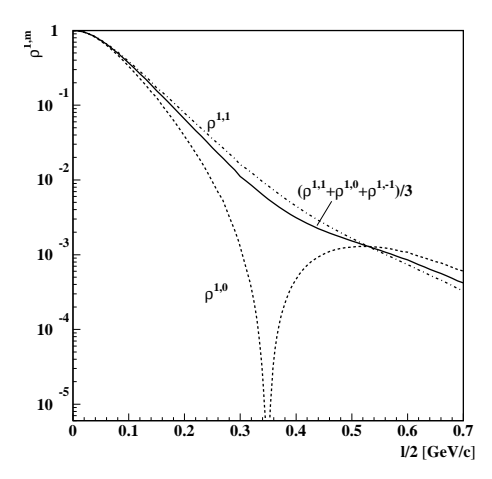


Figure 7. The deuteron density matrix $\rho^{1,m}$ for a spin quantization axis parallel to the photon momentum **q**. The dashed and dash-dotted lines correspond to spin projections m=0 and m=1, respectively. The density matrix for an unpolarized deuteron is shown by the solid curve.

tribution for d(e, e'V)d' reaction for transversely polarized deuteron target at $-t \approx 0.5 \text{ GeV}^2$. Therefore one expects that at these t the cross section should exhibit strong sensitivity to the dynamics of re-interaction of h with the spectator nucleon. This situation gives us a clue on where to look for the CT effects that reveal themselves through the decrease of FSI contribution (Fig.6(b)) with an increase of Q^2 .

In Fig.8 we estimate the expected CT effects for different values of Q^2 based on QDM model of CT¹¹ discussed in the previous section. As Fig.8 demonstrates the onset of CT will result in qualitative changes in the t dependence of the cross section with minimum at $-t \approx 0.45 - 0.5 \text{ GeV}^2$ which becomes increasingly pronounced with an increase of Q^2 .

Note that the very same method of isolating FSI contribution in d(e,e'V)d' reaction at $Q^2\approx 0$ can be used to determine the interaction cross sections of vector mesons with nucleons. This is especially important for ϕ and ψ mesons whose interaction cross section with the nucleon is poorly known¹⁴.

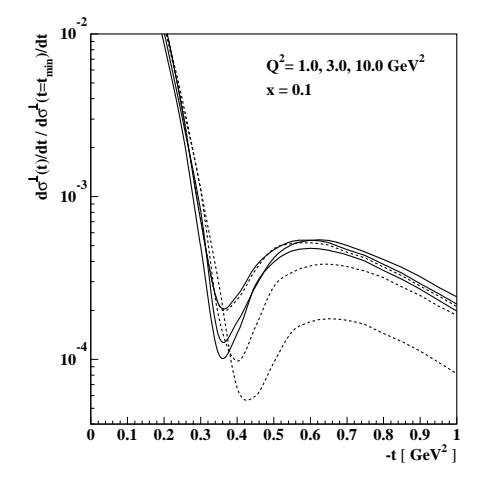


Figure 8. The cross section $d\sigma_{\gamma^*N}^{\perp}/dt$ normalized to its value at $t=t_{min}$. The solid lines present the complete vector meson dominance calculation. Results from quantum diffusion are shown by the dashed curves. The cross sections decrease with an increase of Q^2 .

4. Measurement of Polarized DIS Structure Function of the Neutron

So far we were interested in isolating the D wave contribution of the deuteron wave function which allowed to increase the sensitivity to the short distance phenomena in the reaction involving polarized deuteron. Now we concentrate on the separation of S wave contribution which will give a possibility to estimate the polarized structure function of the "free" neutron. Since the deuteron has a spin 1, in the S state one has simplified relation between helicity of the deuteron and the bound neutron. To isolate these neutrons in almost free state one considers semi-inclusive $e+d \rightarrow e'+p+X$ reaction in which the protons are detected in the target fragmentation region. Such reaction would be very natural for the electron ion collider in the $e\vec{D}$ mode. By selecting only the slowest recoil protons one should be able to isolate the situation whereby the virtual photon scatters from a nearly on-shell neutron in the deuteron. In this way one may hope to extract the DIS structure functions of the neutron with a minimum of uncertainties arising from modeling nuclear effects in the deuteron. As an example we consider the extraction of g_1^n function from $\vec{d}(\vec{e}, e'p)X$ reaction in which the deuteron is polarized in the direction opposite to the direction of incoming electron. In this case the asymmetry with respect to the helicity of incoming electron in the Bjorken limit can be expressed as follows:

$$\sigma^{\uparrow} - \sigma^{\downarrow} \approx \frac{2\alpha_{em}^2}{mx(2-\alpha)Q^4} (1-y) \cdot g_{1n}^{\text{eff}} \left(\frac{x}{2-\alpha}, Q^2\right) \cdot \left[u(p)^2 - \frac{w(p)^2}{2}\right] \tag{10}$$

where $\sigma^{\uparrow(\downarrow)} \equiv \frac{d\sigma^{\uparrow(\downarrow)}}{d\phi dx dQ^2 d(\log \alpha) d^2 p_{\perp}}$ in which \uparrow (\downarrow) corresponds to positive (negative) helicities of incoming electron. For the asymmetry, in Eq.(10, the relativistic corrections due to the Fermi motion are known to be small up to $x \sim 0.5$. In this region the deuteron to a very good approximation will reduce the asymmetry by the depolarization factor of $1 - 3/2P_D$ ¹⁵, where P_D is the total probability of the D state in the deuteron. The example of relativistic description of the density matrix in calculation of g_1d is given in Refs.^{15,16}. It is worth noting that the measurement of g_{1n} using inclusive scattering off the deuteron has certain disadvantages - one has to subtract g_{1p} which is larger in a wide x range, and there is a question of the EMC type effects. Hence to extract the free g_{1n} in a model independent way one would tag spectator protons (a rather easy task for the collider kinematics) and perform the measurements at $p \to 0$

To extract the free g_{1n} from Eq.(10) one first measures the limit of $p \to 0$. Since the D wave vanishes in this limit we are sensitive only to the S partial wave. Furthermore, we can extrapolate the measured tagged neutron structure g_{1n}^{eff} to the region of negative values of kinetic energy of the spectator proton¹⁷. This method is analogous to the Chew–Low procedure for extraction of the cross section of scattering off a pion¹⁸. Such an extrapolation allows us to isolate the pole in the S wave which corresponds to the on-shell neutron interacting with virtual photon. This pole in the IA amplitude is located at $E_{kin}^{pole} = -\frac{|\epsilon_D| - (m_n - m_p)}{2}$. The advantage of this approach is in the fact that the scattering amplitudes containing final state interactions do not have singularities corresponding to on-shell neutron states. Thus, isolating the singularities through the extrapolation of effective structure functions into the negative spectator kinetic energy range will suppress the FSI effects in the extraction of the free DIS structure function.

5. Outlook

Use of the polarized deuteron targets in high energy electro-production reaction gives unique possibility to study the strong interaction at short space-time distances. These studies are the part of the broad program dedicated to the investigation of the structure of deeply bound nucleon as well as the physics of color transparency¹⁷. In semi-inclusive DIS reactions with low momenta of recoil protons the use of the polarized deuterons allow

to perform very accurate measurements of polarized structure functions of the neutron. This program could benefit tremendously from the advances of the building the polarized deuteron targets that can be operated under the high current electron beams as well as from building the polarized electron -ion collider.

References

- L. L. Frankfurt, W. R. Greenberg, G. A. Miller, M. M. Sargsian, M. I. Strikman, Z. Phys. A352, 97 (1995); Phys. Lett. B369, 201 (1996).
- L. L. Frankfurt, M. M. Sargsian, M. I. Strikman, Phys. Rev. C 56, 1124 (1997).
- 3. M. M. Sargsian, Int. J. Mod. Phys. E 10, 405 (2001).
- 4. In plane wave impulse approximation, in which only the diagram of Fig.(2)(a) is included, the $S_d^{\vec{s}}(q, p_p, p_n)$ represents the probability for the proton in the polarized deuteron to have a momentum p_m .
- L. L. Frankfurt and M. I. Strikman, (a) Phys. Rep. 76, 217 (1981); (b) 160, 235 (1988).
- W. Melnitchouk, A. W. Schreiber, and A. W. Thomas, Phys. Rev. **D49**, 1183 (1994).
- 7. T. de Forest, Nucl. Phys. **A392**, 232 (1983).
- 8. E. M. Aitala et al. [E791 Collaboration], Phys. Rev. Lett. 86, 4773 (2001).
- 9. L. Frankfurt, G. A. Miller and M. Strikman, Phys. Lett. B 304, 1 (1993).
- L. L. Frankfurt, G. A. Miller and M. I. Strikman, Ann. Rev. Nucl. Part. Phys. 44, 501 (1994).
- G. R. Farrar, L. L. Frankfurt, M. I. Strikman and H. Liu, Phys. Rev. Lett. 61, 686 (1988).
- L. L. Frankfurt, W. R. Greenberg, G. A. Miller and M. I. Strikman, Phys. Rev. C46, 2547 (1992).
- 13. L. Frankfurt, W. Koepf, J. Mutzbauer, G. Piller, M. Sargsian and M. Strikman, Nucl. Phys. A 622, 511 (1997).
- L. Frankfurt, G. Piller, M. Sargsian and M. Strikman, Eur. Phys. J. A 2, 301 (1998)
- 15. L. L. Frankfurt and M. I. Strikman, Nucl. Phys. A 405, 557 (1983).
- 16. N. L. Ter-Isaakian, Phys. Lett. B 381, 331 (1996).
- 17. M.M. Sargsian, J. Arrington et al, arXiv:nucl-th/0210025.
- 18. G.F. Chew and F.E. Low, Phys. Rev. 113 1640 (1959).